Available online at www.sciencedirect.com
SCIENCE DIRECT®
Biochemical Pharmacology 67 (2004) 1445–1457
Biochemical Pharmacology
www.elsevier.com/locate/biochempharm

Arachidonic and eicosapentaenoic acid metabolism by human CYP1A1: highly stereoselective formation of 17(*R*),18(*S*)-epoxyeicosatetraenoic acid

Dieter Schwarz[a,*], Pyotr Kisselev[b], Spencer S. Ericksen[c], Grazyna D. Szklarz[c], Alexey Chernogolov[a,1], Horst Honeck[d], Wolf-Hagen Schunck[d], Ivar Roots[a]

[a]*Institute of Clinical Pharmacology, University Medical Center Charité, Humboldt University of Berlin, Schumannstrasse 20-21, Berlin 10098, Germany*
[b]*Institute of Bioorganic Chemistry, Academy of Sciences of Belarus, Minsk 220141, Belarus*
[c]*Department of Basic Pharmaceutical Sciences, School of Pharmacy, West Virginia University, Morgantown, WV 26505, USA*
[d]*Max Delbrueck Center for Molecular Medicine, Berlin 13125, Germany*

Received 27 August 2003; accepted 1 December 2003

Abstract

Human cytochrome P450 1A1 (CYP1A1) and human NADPH-cytochrome P450 reductase were expressed and purified from *Spodoptera frugiperda* insect cells. A reconstituted enzymatically active system metabolized polyunsaturated fatty acids such as arachidonic (AA) and eicosapentaenoic acid (EPA). CYP1A1 was an AA hydroxylase which oxidizes this substrate at a rate of 650 ± 10 pmol/min/nmol CYP1A1, with over 90% of metabolites accounted for by hydroxylation products and with 19-OH-AA as major product. Epoxyeicosatrienoic acid (EET), mainly 14,15-EET, accounted for about 7% of total metabolites. Unlike rat CYP1A1, the human enzyme exhibited no 20-OH-AA as product. In contrast, with EPA as substrate CYP1A1 was mainly an epoxygenase, oxidizing with over 68% of total metabolites EPA to 17(*R*),18(*S*)-epoxyeicosatetraenoic acid (17(*R*),18(*S*)-EETeTr). 19-OH-EPA accounted for about 31% of total metabolites. Significantly, the 17,18-olefinic bond of EPA was epoxidized to 17(*R*),18(*S*)-EETeTr with nearly absolute regio- and stereoselectivity. Molecular modeling analyses provided rationale for high efficiency of AA hydroxylation at C_{19} and its gradual decrease down to C_{14}, as well as for the limited EPA 17(*S*),18(*R*) epoxidation due to unfavorable enzyme–substrate interactions. The absence of ω-hydroxylation for both substrates is not due to steric factors, but probably a consequence of different reactivities of ω and $(\omega - 1)$ carbons for hydrogen abstraction. It is suggested that the capacity of human CYP1A1 to metabolize AA and EPA and its inducibility by polycyclic aromatic hydrocarbons may affect the production of physiologically active metabolites, in particular, in the cardiovascular system and other extrahepatic tissues including lung.

Keywords: Human cytochrome P450 1A1; CYP1A1; Polyunsaturated fatty acid; Arachidonic acid; Eicosapentaenoic acid; Vasoactive metabolite

1. Introduction

AA can be metabolized by CYP enzymes to several classes of oxygenated metabolites. The product profile depends on the CYP isoform involved and may consist of a series of regio- and stereoisomeric EETs and hydroxyeicosatetraenoic acids (midchain HETEs and 16- through 20-OH-AA) [1]. Several of these CYP-derived eicosanoids have potent biological activities and are increasingly recognized to play important roles in the regulation of vascular tone and of renal, pulmonary, and cardiac function (reviewed in [2–6]). Human CYP isoforms acting primarily

* Corresponding author. Tel.: +49-30-450525004; fax: +49-30-450525933.
E-mail address: dieter.schwarz@charite.de (D. Schwarz).
[1] On leave from the Research Institute for Physical and Chemical Problems, Belarussian State University, Minsk, Belarus. Present address: Research Institute for Molecular Pharmacology, 13125 Berlin-Buch, Germany.

Abbreviations: CYP, cytochrome P450; CYP1A1, human cytochrome P450 1A1; P450 reductase, human NADPH cytochrome P450 reductase; Sf9, *Spodoptera frugiperda* insect cells; AA, arachidonic acid (eicosatetraenoic acid); EPA, eicosapentaenoic acid; EET, epoxyeicosatrienoic acid; HETE, hydroxyeicosatetraenoic acid; EETeTr, epoxyeicosatetraenoic acid; RP-HPLC, reversed-phase HPLC; NP-HPLC, normal-phase HPLC.

0006-2952/$ – see front matter © 2004 Elsevier Inc. All rights reserved.
doi:10.1016/j.bcp.2003.12.023

as AA epoxygenases include CYP1A2, CYP2C8, CYP2C9 and CYP2J2 [7–9]. Some of these EET-generating CYP isoforms additionally yield midchain HETEs by bisallylic hydroxylations [10]. In contrast, CYP4A11, CYP4F2 and CYP4F3 act as AA ω-hydroxylases and produce 20-OH-AA (20-HETE) in human liver and kidney [11–13].

EPA (20:5, N − 3), another polyunsaturated fatty acid, shares with AA (20:4, N − 6) the same number of carbon atoms but contains an additional double bond between C_{17} and C_{18}. Thus, EPA is an (ω − 3) polyunsaturated fatty acid whereas AA is of the (ω − 6) type. EPA may serve as an alternative substrate in CYP-dependent epoxygenation and hydroxylation reactions as shown with rat hepatic and renal microsomes [14]. However, specific CYP isoforms involved in EPA metabolism have not been identified till date, and the biological activities of the metabolites are only partially known. Recent studies demonstrated that EPA epoxides share and even exceed the ability of AA epoxides to stimulate calcium-activated potassium (BK) channels in vascular smooth muscle cells [15], to activate cardiac ATP-sensitive potassium channels [16] and to mediate vasodilation [17]. CYP epoxygenase metabolites of docosahexaenoic acid, another major (ω − 3) type fatty acid, were shown potent dilators of coronary arterioles and importantly more potent than EETs in activating BK channels [18].

CYP1A1 is one of the key enzymes in the metabolism and activation of procarcinogenic xenobiotics such as polycyclic aromatic hydrocarbons and other environmental pollutants [19–22]. CYP1A1 is constitutively expressed and/or highly inducible by ligands of the aryl hydrocarbon receptor in the lung, gastro-intestinal tract, placenta, brain, and in vascular endothelial and smooth muscle cells [23–27]. Whereas its role in xenobiotics metabolism is widely recognized, at present it is discussed that human CYP1A1 might also have important—partially unknown—endogenous ligands. Particularly, steroids and retinoids have been reported to be endogenous substrates [28–30]. To our knowledge, there are no reports showing the ability of the human CYP1A1 to metabolize polyunsaturated fatty acids such as AA and EPA. However, AA metabolism was detected with several other members of the CYP1A subfamily, e.g. purified rabbit and rat CYP1A1 as well as rat CYP1A2 [31,32]. Human CYP1A2 and chicken CYP1A5 act predominantly as AA epoxygenases [7,33]. Moreover, studies in rodent, chicken and fish models revealed species-specific alterations in microsomal AA metabolism in response to treatments with polycyclic aromatic hydrocarbons acting as CYP1A inducers, consistent with the ability of various CYP1A enzymes to metabolize AA; note that another member of CYP1 family, CYP1B1, is also inducible and may contribute to the metabolism of fatty acids [32,34,35].

In the present study, we addressed the question whether human CYP1A1 with known expression and inducibility in the vasculature is able to metabolize AA and EPA. To this end, human CYP1A1 and human P450 reductase were heterologously expressed in Sf9 insect cells, purified and reconstituted into the microsomal membrane of Sf9 control microsomes to yield an enzymatically active system. The results show that human CYP1A1 towards AA exhibits mainly hydroxylase activity with distinct differences in regioselectivity compared to rat CYP1A1. Towards EPA as substrate it is an epoxygenase with a remarkable high degree of regio- and stereochemical selectivity in favor of the formation of 17(*R*),18(*S*)-EETeTr, a novel vasoactive metabolite. Molecular modeling of CYP1A1–fatty acid interactions was then used to rationalize the observed regio- and stereospecificity of AA and EPA oxidation by human CYP1A1.

2. Materials and methods

2.1. Materials

AA and EPA were purchased from Cayman Chemical. [1-^{14}C]AA (56 mCi/mmol) was from Amersham Pharmacia Biotech and [1-^{14}C]EPA (55.6 mCi/mmol) from NEN Life Science. All other chemicals were obtained in the purest commercially available form.

Reference compounds for HPLC analysis: EETs were purchased from Cayman Chemical. 19-OH- and 20-OH-EPA were generated enzymatically by NADPH-dependent oxygenation of [1-^{14}C]EPA with rat kidney microsomes, the regioisomeric mixture was collected from RP-HPLC, and both isomers separated by subsequent NP-HPLC as described [15]. 19-OH- and 20-OH-AA were generated analogously. Regioisomeric EPA epoxides were synthesized chemically followed by subsequent RP-HPLC to separate and collect the 17,18-EETeTr. The identity of the 17,18-EETeTr was confirmed by hydrolysis and subsequent GC-MS analysis as described [15]. A mixture of both enantiomers of 17,18-EETeTr's was also produced using CYP4A1 microsomes and used as standard in coelution chiral-phase HPLC runs. Recombinant baculovirus for the CYP4A1 expression was kindly provided by Dr. M.L. Schwartzman. Recombinant human cytochrome b_5 was purchased from Oxford Biomedical Research. Bacterial CYP102 was a gift of Dr. R. Schmid.

2.2. Expression and purification of human CYP1A1 and human P450 reductase

The modified CYP1A1 cDNA was constructed previously [30]. The enzyme was expressed in Sf9 insect cells as C-terminal His-tag protein and purified by Ni-affinity chromatography as described [30]. Human P450 reductase was expressed in Sf9 cells and purified as described [36]. Recombinant baculovirus for expression of P450 reductase in Sf9 cells was kindly provided by Dr. F.J. Gonzalez. Sf9 control microsomes were prepared from

Sf9 cells not transfected with any baculovirus as described for the recombinant baculovirus-infected cells [37].

CYP content was measured by sodium dithionite reduced-CO minus reduced difference spectroscopy [38]. Protein concentration was determined by Coomassie Plus protein assay (Pierce). P450 reductase concentration was determined spectrally using an extinction coefficient of 21.2 $mM^{-1}\,cm^{-1}$ (at 455 nm) [36]; P450 reductase activity was determined from the rate of cytochrome *c* reduction [39].

2.3. Arachidonic and eicosapentaenoic acid assay

In standard AA assays, purified human CYP1A1 was combined with purified human P450 reductase and Sf9 control microsomes; mixtures contained 2.5 μM CYP1A1, 6.25 μM reductase and 20 mg/mL microsomes in 10 μL buffer (50 mM Tris–HCl, pH 7.5, 100 mM NaCl) and were incubated for 10 min on ice ('reconstituted CYP1A1+ reductase microsomes'). The volume was adjusted with buffer to 490 μL followed by addition of 4.5 nmol [1-^{14}C]AA plus the corresponding amount of ''cold'' AA in 5 μL of 100 mM Tris–HCl, pH 8.0 to give 20–100 μM final substrate concentration (total volume 500 μL). After pre-incubation for 3 min at 37°, reactions were started by the addition of 5 μL of NADPH (100 mM) and carried out for 15 min at 37°. After quenching the reactions with 25 μL of citric acid (0.4 M), products and residual substrate were extracted twice with ethyl acetate using 2.5 mL aliquots. Solvent was evaporated under a stream of nitrogen, products were reconstituted in ethanol and analyzed by HPLC.

EPA assays were carried out as described above for AA using however 3.75 nmol [1-^{14}C]EPA (corresponding to 4.63×10^5 dpm) plus the corresponding amount of ''cold'' EPA in 5 μL of 100 mM Tris–HCl, pH 8.0, buffer in a total final volume of 250 μL giving final substrate concentrations of 15–92 μM.

2.4. HPLC and product characterization

A HPLC system (LC-10Avp, Shimadzu) equipped with a radioactivity detector (LB509, Berthold) and the following columns was used: Nucleosil 100-5C18HD (250 mm× 4 mm) for RP-HPLC, Nucleosil 100-5 (250 mm × 4 mm) for NP-HPLC (both from Macherey-Nagel) and a Chiralcel OB (250 mm × 4.6 mm) for chiral HPLC (from Daicel). RP-HPLC was performed with a linear gradient of acetonitrile/water/acetic acid (50:50:0.1, v/v/v) to acetonitrile/acetic acid (100:0.1, v/v) over 40 min at a flow rate of 1 mL/min. The hydroxylation products, 19/20-OH-AA eluted between 14.5 and 15.75 min and 19/20-OH-EPA eluted between 12.5 and 15 min, respectively, from the RP-HPLC column. The fractions from several separations were combined and resolved further by NP-HPLC using a linear gradient from hexane/2-propanol/acetic acid (99:1:0.1, v/v/v) to hexane/2-propanol/acetic acid (98.3:1.7:0.1, v/v/v) over 40 min at a flow rate of 1 mL/min. Fractions containing 16/17/18-OH-AA were collected as batches from the RP-HPLC column between 15.75 and 17.5 and separated by NP-HPLC as described [32].

The enantiomers of 17,18-EETeTr eluting from the RP-HPLC column between 17.5 and 20 min were collected in batches and resolved by chiral HPLC using a linear gradient from hexane/2-propanol (99.7:0.3, v/v) to hexane/2-propanol (98:2, v/v) at a flow rate of 1 mL/min. Prior to chiral HPLC, the epoxyeicosatetraenoic acid enantiomers were esterified with diazomethane as described [40].

The *y*-axis of all HPLC chromatograms represents the response of the radioactive monitor (1 V corresponds to 5×10^4 cpm). Using about 2×10^5 cpm radioactivity (corresponding to about 2 nmol substrate), we estimate the sensitivity for detection of products to be at least 0.2% of total activity (peak area).

2.5. Molecular modeling

Computer modeling was performed using InsightII/Discover software (Accelrys, Inc.) on an SGI Octane workstation with MIPS R10000 (CPU)/MIPS R10010 (FPU) processors. The consistent valence force field was employed for all molecular modeling simulations and the parameters for heme and ferryl oxygen were as described earlier [41,42]. The homology model of CYP1A1 was constructed earlier based on the crystal structure of CYP2C5 [43].

Substrates AA and EPA were constructed using the Builder module and positioned in the active site of the homology model, based on the proposed binding orientation of fatty acids in cytochrome P450 BM-3 [44]. The orientation of each substrate was then adjusted manually to enable fatty acid oxidation at various positions leading to observed products. For both AA and EPA, the individual productive binding orientations examined were those leading to oxidations at C_{14} through C_{20} on the hydrocarbon tail of the substrate. Each of the enzyme–substrate complexes formed was then optimized by a combination of minimization and molecular dynamics performed on the substrate and protein residues within 5 Å from the compound. Initially, the complex was minimized using the steepest descent method until a maximum RMS derivative of 1 kcal/mol/Å was achieved. To assure the correct substrate orientation during the subsequent molecular dynamics simulations, half-harmonic force restraints were imposed between the ferryl oxygen and carbon atoms from C_{14} to C_{20}. Each restraint drew a particular site of oxidation on the substrate into proximity of the activated heme oxygen as a means to bias the sampling in the molecular dynamics simulation toward particular, catalytically-relevant enzyme–substrate configurations. Thus, for hydroxylation reactions, the restraint between the atoms restricted the maximum interatomic distance to about 5 Å to promote hydrogen abstraction, while in the case of 17(*R*),18(*S*) epoxidation of EPA, C_{17} and C_{18} were restricted to a distance of about 3 Å to allow for that reaction to occur.

Each restrained complex underwent 1 ps of molecular dynamics at 300 K, *in vacuo*, followed by steepest descent minimization, as described earlier [45–48]. The energy of the system and non-bond enzyme–substrate interaction energies were calculated for each complex.

To assess the stability of each of the productive substrate binding orientation, unrestrained molecular dynamics simulations were performed for 5 ps at 300 K *in vacuo*, in which both the substrate and active site residues within 5 Å from the substrate were allowed to move [48,49]. The results were analyzed and plots were generated using the Analysis module of InsightII.

3. Results

3.1. Expression and reconstitution

Human CYP1A1 was expressed as a spectrally and functionally active enzyme with the C-terminus extended by six His residues. The purified protein had a specific CYP content of 11.2 nmol/mg protein and was electrophoretically homogenous as observed from SDS-PAGE. Reduced CO-difference spectroscopy proved the expressed enzyme to be free of any inactive cytochrome P420 (not shown). P450 reductase purified to a specific catalytic activity of 18.2 U/mg protein and was electrophoretically homogenous according to SDS-PAGE. Reconstitution of enzymatic activity, based on the purified enzymes, CYP1A1 and P450 reductase, was achieved by incubation with Sf9 control microsomes. The control microsomes contained no CYP as indicated by both the CO difference spectrum and lack of activity towards several substrates such as ethoxyresorufin, benzo[*a*]pyrene, AA and EPA. High catalytic activity of this reconstituted CYP1A1 system was demonstrated for EROD, benzo[*a*]pyrene hydroxylation, and 7,8-dihydrodiol-benzo[*a*]pyrene epoxidation establishing the enzymatic competence of this approach and its utility for analysis of AA and EPA metabolism (not shown). To establish conditions for optimal CYP1A1 catalytic activity, the effect of varying amounts of both P450 reductase and cytochrome b_5 on the AA oxidation reaction was studied. The results indicated that a 2.5-fold molar excess of P450 reductase over CYP1A1 is sufficient for near optimal activity of CYP1A1. Inclusion of cytochrome b_5 in the preincubation mixture up to 2-fold molar excess over P450 reductase had no effect on CYP1A1 activity supporting earlier reports on the absence of stimulating effects of cytochrome b_5 on EROD and benzo[*a*]pyrene hydroxylation [37,50].

3.2. Arachidonic acid metabolism, product identification and distribution

The RP-HPLC separation of AA oxidation products generated by human CYP1A1 led to major peaks containing various primary metabolites: 19-/20-hydroxylated AA eluting with a retention time of 14.8 min, a mixture of 16-/17-/18-hydroxylated AA eluting in the broad peak (with a shoulder) immediately after 19-/20-OH-AA with a retention time around 16.1 min, and AA epoxides eluted with retention times between 22 and 25 min (Fig. 1A). A subsequent analysis using authentic standards provided means to identify the larger peak as 14,15-EET (retention time: 23.0 min). The smaller peak eluting at 24.2 min probably represents a small amount of 11,12-EET and/or 8,9-EET as proved by coelution of the corresponding standards. The product peak at 14.8 min was further analyzed by NP-HPLC and consisted of solely 19-OH-AA eluting at 23.3 min (Fig. 1B, upper trace). The products eluting from RP-HPLC column between 15.75 and 17.5 min were collected and rechromatographed by NP-HPLC yielding three resolved components (Fig. 1C). Based on analysis described in detail previously [32], these metabolites were identified as 17-OH-AA, 18-OH-AA, and 16-OH-AA (retention times: 39.2, 42.6, and 45.0 min, respectively). The approximate relative distribution of 17-, 18-, and 16-OH-AA was 16, 56, and 28%, respectively. The minor peak at about 29 min (Fig. 1A, upper trace) remained unidentified; its area corresponds to less than 10% activity compared with the major peaks of hydroxylated products and it was not considered in the analysis below.

Catalytic rates of purified human CYP1A1-catalyzed AA metabolism were determined at three different AA concentrations, namely 20, 50, and 100 μM. The rates measured at 100 μM were not much higher compared to those at 50 μM demonstrating nearly saturating substrate level at the highest concentration. Moreover, the analysis showed that the profile of metabolites remained constant over that region of substrate concentration. Total rates and the regioselectivity of purified human CYP1A1-catalyzed AA metabolism are shown in Table 1. With a total metabolic rate of 650 pmol product/min/nmol of CYP1A1 and

Table 1
Total rates and product distribution in AA oxidation by human CYP1A1

	Rate (pmol/min/nmol CYP1A1)	Product distribution (%)
Total rate	650 ± 100	100
20-OH-AA	0	0
19-OH-AA	270 ± 30	42
18-OH-AA	180 ± 30	28
17-OH-AA	50 ± 10	8
16-OH-AA	90 ± 20	13.8
14,15-EET	40 ± 10	6
Other EET	≤10	1

CYP1A1 was incubated with P450 reductase, Sf9 control microsomes, and AA (final concentration: 50 nM, 250 nM, 200 μg of microsomal protein/mL, and 100 μM, respectively). Reaction proceeded and products were extracted and analyzed as described in Section 2. Regiospecificity of hydroxylation was determined by normal-phase HPLC, respectively as described in Section 2. The rate values represent means ± SD calculated from three different experiments.

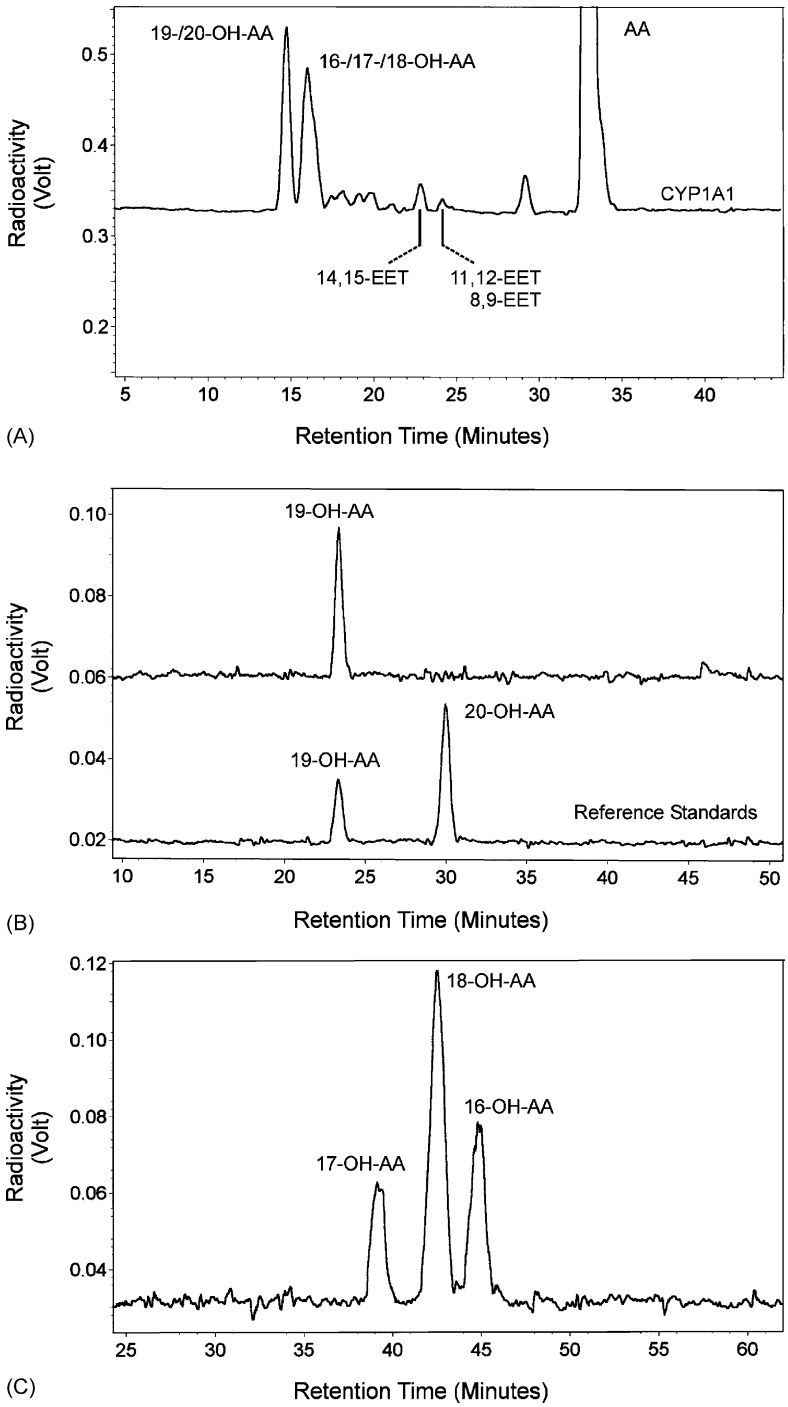

Fig. 1. HPLC of AA metabolism by human CYP1A1. (A) Reversed-phase HPLC with the hydroxylation products, 19-/20-OH-AA, eluting at 14.8 min and 16-/17-/18-OH-AA, eluting at 16.1 min, and several EETs between 22 and 25 min. Standard EET compounds eluted at the indicated retention times. (B) Normal-phase HPLC resolution of the 19-, and 20-OH-AA metabolites. The peak eluting between 14.5 and 15.75 min in RP-HPLC was collected from three reactions and rechromatographed by NP-HPLC. The lower trace showed the separation of a mixture of reference 19-OH- and 20-OH-AA, eluting at 23.3 and 30.0 min, respectively, proving that the initial peak in RP-HPLC consisted solely of 19-OH-AA. (C) Normal-phase HPLC resolution of the 16-, 17-, and 18-OH-AA metabolites. The broad peak eluting between 15.75 and 17.5 min in RP-HPLC was collected and rechromatographed by NP-HPLC. Identification of the three resolved components eluting at 39.2, 42.6, and 45.0 min, respectively, was based on similarity to the NP-HPLC resolution of these metabolites shown in Fig. 2 in the paper of Falck *et al.* [32]. The *y*-axis of all chromatograms represents the response of the radioactive monitor (1 V corresponds to 5×10^4 cpm). For other conditions see Section 2.

more than 90% hydroxylation products, nearly one half of total CYP1A1 hydroxylase activity is directed to produce 19-OH-AA. No 20-OH-AA product (ω-hydroxylation activity) was identified. The monohydroxylated metabolites 18-, 17-, and 16-OH-AA were formed in an approximate 2:0.6:1 molar ratio (Table 1), comprising 28, 8, and 13.8% of the product profile, respectively. On the other hand, CYP1A1 is not an efficient AA epoxygenase, with

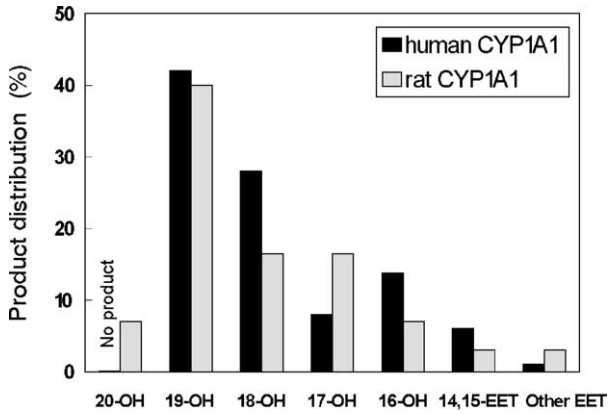

Fig. 2. Product profiles in AA metabolism by human and rat CYP1A1. Data for rat CYP1A1 were taken from Falck *et al*. [32]. No product: human CYP1A1 exhibited no ω-hydroxylation.

EET formation only accounting for about 7% of total metabolites. In Fig. 2, a direct comparison of product profiles in AA metabolism by human and rat CYP1A1 is shown (data for rat CYP1A1 were taken from [32]).

3.3. Eicosapentaenoic acid metabolism, product identification and distribution

Incubations of EPA with purified CYP1A1 in the presence of purified P450 reductase and control microsomes resulted in NADPH-dependent formation of two main metabolites with RP-HPLC retention times of 13.3 and 18.8 min, respectively (Fig. 3A, upper trace). Control microsomes devoid of any P450 were inactive (Fig. 3A, lower trace). Hydroxylated EPA products eluted with a retention time of 13.3 min in RP-HPLC. Rechromatography and further analysis by NP-HPLC demonstrated that this peak contained solely 19-OH-EPA (retention time: 20.4 min), with no 20-OH-EPA present (Fig. 3B). CYP1A1 was also able to epoxidize EPA as shown by the presence of metabolites with a retention time of 18.8 min in RP-HPLC (Fig. 3A) co-migrating with chemically synthesized 17,18-EETeTr. Other regioisomeric EPA epoxides migrating with retention times between 20 and 21 min in RP-HPLC were not detectable. To analyze the stereoselectivity of EPA epoxygenation, the products present in this fraction, collected from three RP-HPLC runs, were derivatized to methylesters and subsequently analyzed by chiral-phase HPLC (Fig. 3C). Chiral-phase HPLC resulted in only one peak with a retention time of 22.4 min (Fig. 3C, upper trace). Subsequent analysis of the enantiomeric 17(*R*),18(*S*)- and 17(*S*),18(*R*)-EETeTr synthesized by enzymatic oxidation of EPA by CYP4A1 and bacterial CYP102 [15] provided standards by which the analyte was identified as the 17(*R*),18(*S*)-EETeTr enantiomer (Fig. 3C, lower traces). The minor peak immediately after 19-OH-EPA (designated as ''X'' in RP-HPLC, Fig. 3A) remains unidentified. However, we can exclude any hydroxylated EPA metabolite as proved by NP-HPLC.

Table 2
Total rates and product distribution in EPA oxidation by human CYP1A1

	Rate (pmol/min/nmol CYP1A1)	Product distribution (%)
Total rate	640 ± 100	100
20-OH-EPA	0	0
19-OH-EPA	200 ± 20	31
17(*R*),18(*S*)-EETeTr	440 ± 40	68
17(*S*),18(*R*)-EETeTr	<10	<1
Other EETeTr	Not detected	–

CYP1A1 was incubated with P450 reductase, Sf9 control microsomes, and EPA (final concentration: 50 and 250 nM, 200 μg of microsomal protein/mL, and 92 μM, respectively). Reaction proceeded and products were extracted and analyzed as described in Section 2. Regiospecificity of hydroxylation and absolute configuration of epoxygenation products were determined by normal-phase and chiral-phase HPLC, respectively, as described in Section 2. The rate values represent means ± SD calculated from three different experiments.

As for AA, catalytic rates of purified human CYP1A1-catalyzed EPA metabolism also were determined at three different EPA concentration, namely 15, 53, and 92 μM, whereby no increase in the rate at 92 μM was observed and the profile of EPA metabolites did not significantly change over that region of substrate concentration. As calculated from the peak areas Table 2 shows data of analysis of the total rates, the product distribution and the regio- and enantiomeric composition of the products. The total catalytic rate for EPA metabolism is 640 pmol/min/nmol of CYP1A1. As for AA, no ω-hydroxylation was detected, instead solely (ω − 1)-hydroxylation occurred. The epoxygenation product, the 17(*R*),18(*S*) enantiomer, as major metabolite represents 68%, and the hydroxylation metabolite, the 19-OH-EPA, 31% of the total product corresponding to a ratio of epoxygenase and hydroxylase activities of more than 2:1. As the stereo-analysis of epoxidation products showed, human CYP1A1 exhibited a nearly absolute stereo- and regioselectivity of epoxidation in favor of the 17(*R*),18(*S*) enantiomer. The relative amount of the 17(*S*),18(*R*) enantiomer, if any, was estimated to be less than 1%.

3.4. Molecular modeling of CYP1A1–fatty acid complexes

To explain the observed product profiles, fatty acid substrates were docked in the active site of the CYP1A1 model at different productive binding orientations. Fig. 4 shows AA docked in the active site in an orientation leading to the major product, 19-OH-AA, and Fig. 5 shows EPA docked in an orientation allowing for its 17(*R*),18(*S*) epoxidation. Key amino acids which are within 5 Å of the substrate molecule and thus may interact with the substrates are residues 58, 77–81 and 83 of sheet 1, 106–108 of the B–B′ loop, 111 of helix B′, 122 of the B′–C loop, 228 of helix F, 230 and 234–238 of the F–G loop, 316–321 of helix I, 382 and 385–387 of helix K-sheet 1–4 region, 406 and 408 of sheet 1–3, 455, 497–498 of sheet 4–2. Fatty acid

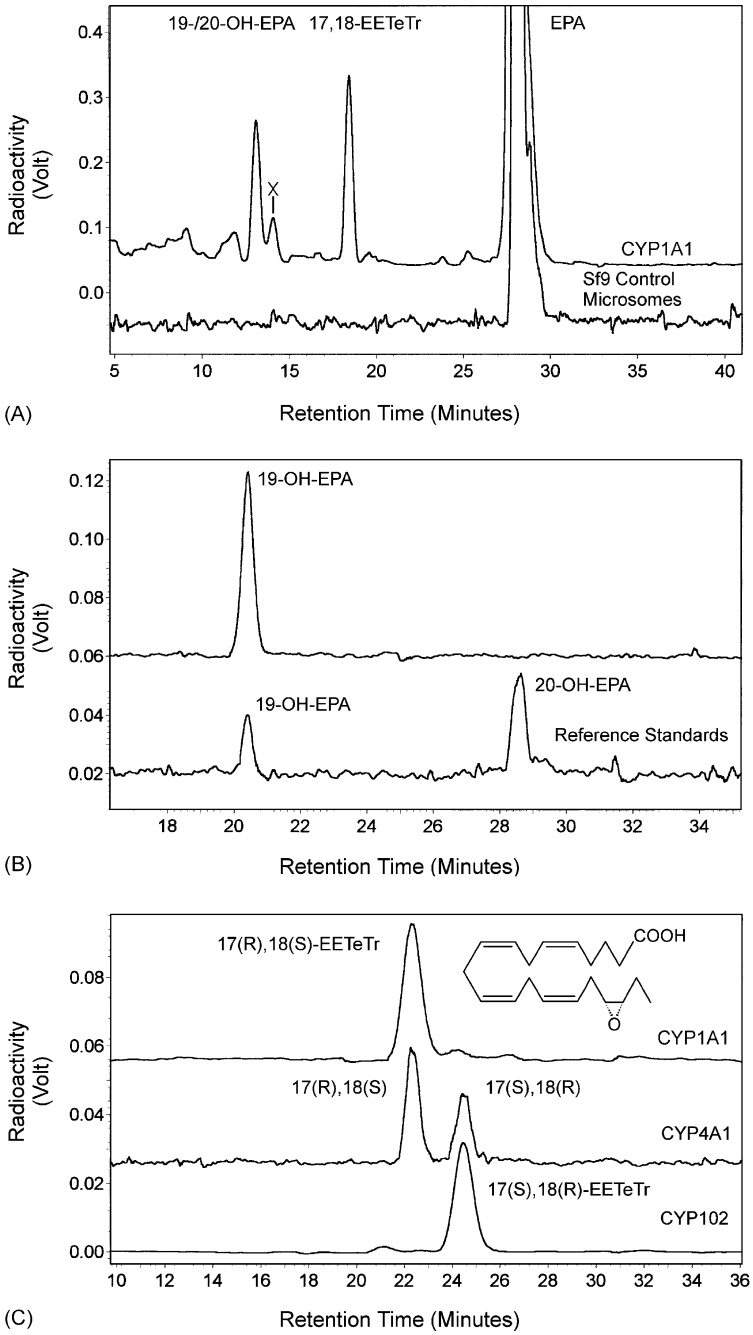

Fig. 3. HPLC of EPA metabolism by human CYP1A1. (A) Reversed-phase HPLC. Upper trace: RP-HPLC with the hydroxylation products, 19-/20-OH-EPA, eluting at 13.3 min and the epoxygenase products, 17,18-EETeTr, eluting at 18.8 min. The lower chromatographic trace shows a control run in which Sf9 control microsomes prepared from uninfected insect cells were used. (B) Normal-phase HPLC resolution of the hydroxylation products. The peak eluting between 12.5 and 15 min in RP-HPLC was collected from three reactions and rechromatographed by NP-HPLC. The lower trace showed the separation of a mixture of reference 19-OH- and 20-OH-EPA, eluting at 20.4 and 28.6 min, respectively, proving that the initial peak in RP-HPLC consisted solely of 19-OH-EPA. (C) Chiral-phase HPLC resolution of the epoxygenase products. The peak eluting between 18 and 19.5 min in RP-HPLC was collected from three reactions, converted to methylester, and analyzed by chiral-phase HPLC. The middle trace is a chromatogram of a mixture of 17(*R*),18(*S*)-EETeTr and 17(*S*),18(*R*)-EETeTr synthesized enzymatically by oxidation of EPA by CYP4A1 (retention times: 22.4 and 24.4 min, respectively). The lowest trace is a chromatogram of 17(*S*),18(*R*)-EETeTr (retention time: 24.4 min) synthesized enzymatically by oxidation of EPA by bacterial CYP102. Both chromatograms prove that the epoxygenase product in the RP-HPLC solely consisted of 17(*R*),18(*S*)-EETeTr. The insert shows the structure of the optically pure enantiomer 17(*R*),18(*S*)-EETeTr. For other conditions see Section 2.

substrates are stabilized in the active site mainly by hydrophobic interactions, although the carboxy terminus is able to form hydrogen bonds with the backbone amide hydrogens of Gly-79, Ser-80 and Thr-81, and with the hydroxyl group of Thr-81. Interestingly, this hydrogen bond network is found for different productive orientations of AA and EPA, and it persists throughout the 5 ps molecular dynamics simulations. Thus, it seems that these

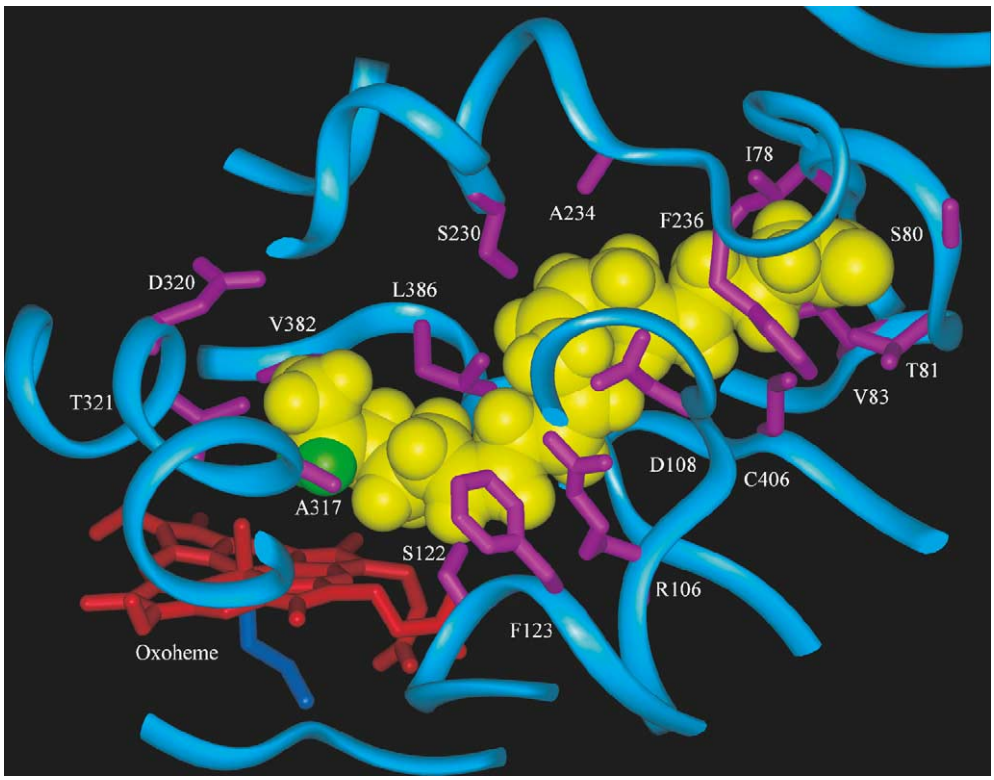

Fig. 4. The active site of the CYP1A1 homology model with AA (yellow) docked in an orientation leading to its hydroxylation at C_{19}. Methylene hydrogens that can be abstracted are shown in green, residues within 5 Å from the substrate are in magenta, and heme and ferryl oxygen are red.

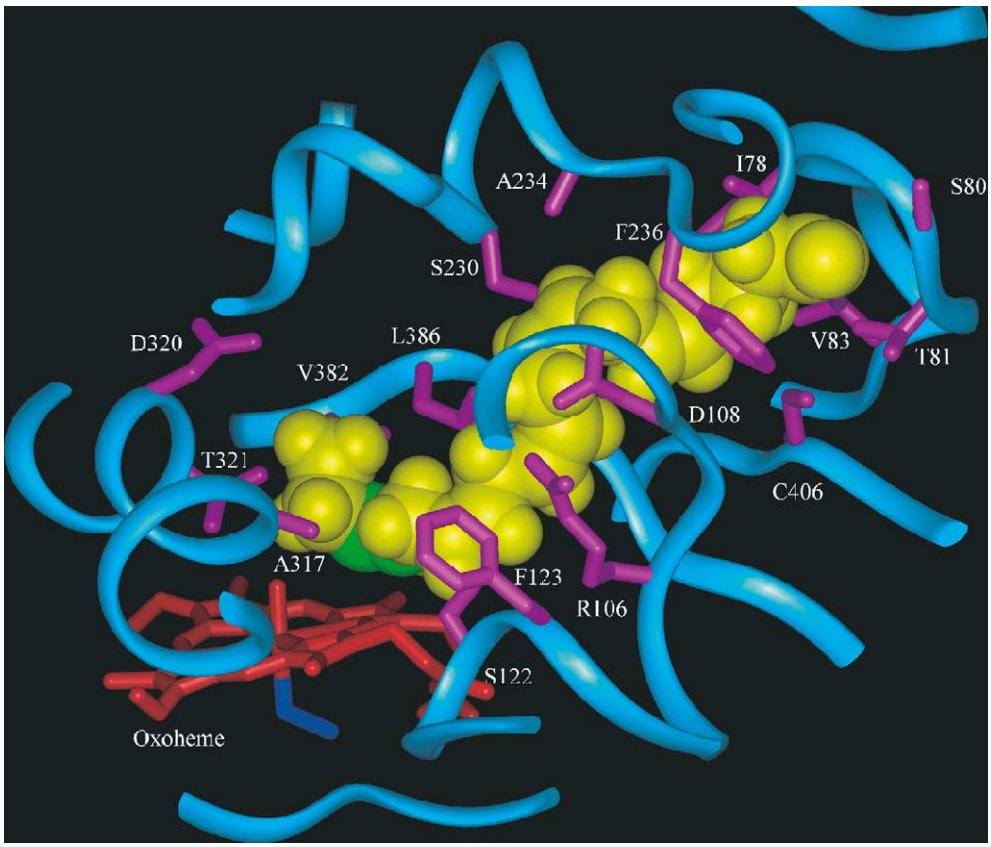

Fig. 5. The active site of the CYP1A1 homology model with EPA (yellow) docked in an orientation leading to its 17(*R*),18(*S*) epoxidation. C_{17} and C_{18} are shown in green, residues within 5 Å from the substrate are in magenta, and heme and ferryl oxygen are red.

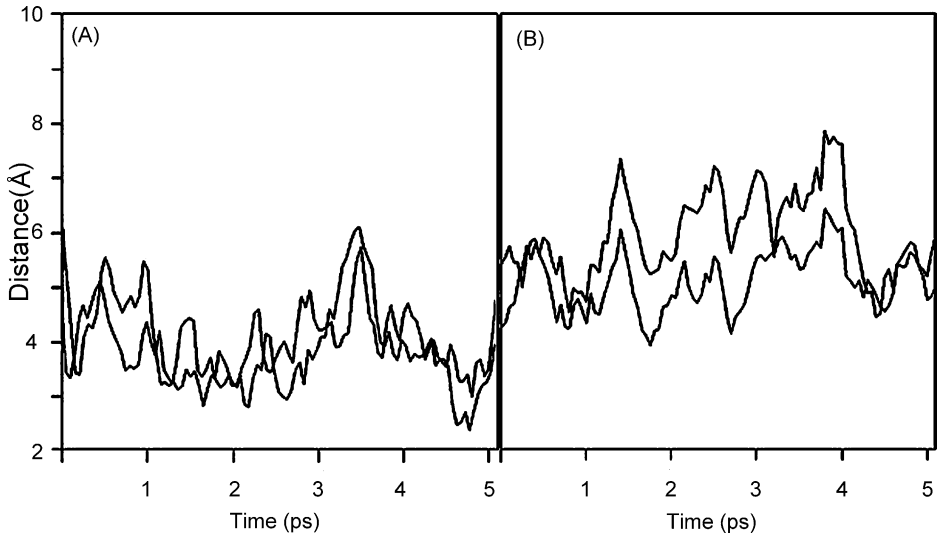

Fig. 6. The distance between the ferryl oxygen and methylene hydrogens at oxidation sites for arachidonate bound in the active site of CYP1A1 plotted as a function of time. (A) Methylene hydrogens at C_{19}—ferryl oxygen distance; (B) methylene hydrogens at C_{17}—ferryl oxygen distance. The simulations were initiated for the substrate bound in the productive binding orientation.

hydrogen bonds play a role in stabilizing the fatty acid molecule in the active site and ensuring its oxidation at the hydrocarbon tail of the substrate.

The analysis of various AA complexes revealed that the enzyme–substrate interaction energies were about −135 kcal/mol energy when the substrate was docked in orientations leading to hydroxylations at C_{19}, C_{18} and C_{17}, and gradually increased for C_{16} and C_{15} to reach −105 kcal/mol for C_{14}. Moreover, molecular dynamics simulations indicated that the most stable binding orientation was that leading to oxidation at C_{19}, which allowed C_{19} methylene hydrogen atoms to remain within 3 Å from the heme oxygen during the 5 ps simulation (Fig. 6A), thus promoting substrate hydroxylation. The hydrogen–oxygen distance was longer for other carbon atoms examined, as illustrated by the case of C_{17}, where methylene hydrogens were at the distance of about 5 Å or more from the heme oxygen (Fig. 6B), thereby hindering substrate hydroxylation. This may explain higher efficiency of AA hydroxylation at C_{19} compared to lower rates obtained for other products. A special case concerns the possibility of substrate hydroxylation at C_{20}. When AA was docked in the active site in an orientation that would allow for this reaction, the energy of the complex and enzyme–substrate interaction energy were similar to that observed for C_{19}. Moreover, the distance between the heme oxygen and hydrogens at C_{20} was often close to 3 Å throughout the 5 ps molecular dynamics simulation.

The analyses similar to those described above were also performed for EPA–CYP1A1 complexes. Interestingly, 17(*R*),18(*S*) epoxidation was confirmed by docking experiments, which showed that the possibility of 17(*S*),18(*R*) epoxidation was limited by severe steric clashes due to van der Waals overlaps with active site residues. Overall, enzyme–substrate interaction energies for the various complexes displayed trends that were analogous to those

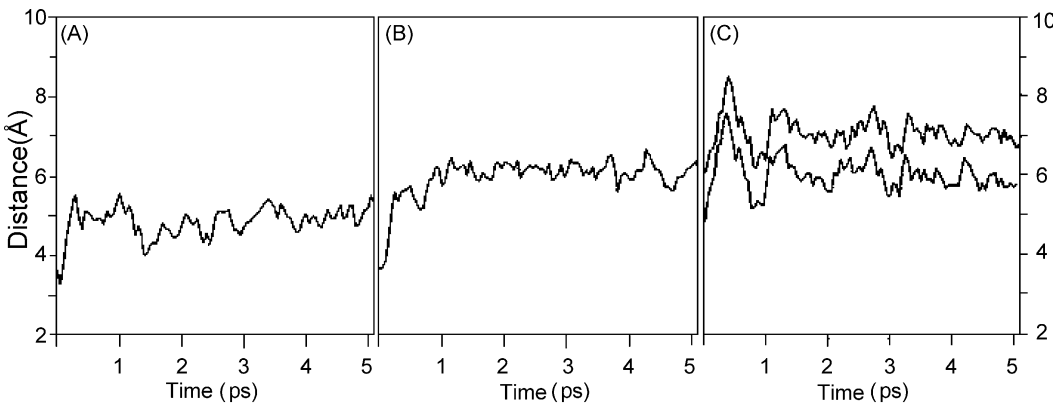

Fig. 7. The distance between the ferryl oxygen and hydrogens or carbons at the oxidation site for eicosapentaenoate bound in the active site of CYP1A1 plotted as a function of time. (A) C_{18}—ferryl oxygen distance; (B) C_{17}—ferryl oxygen distance; (C) methylene hydrogens at C_{16}—ferryl oxygen distance. The simulations were initiated for the substrate bound in the productive binding orientation.

observed with AA. Thus, the interaction energies of the EPA–CYP1A1 complexes were lowest, about −280 kcal/mol, when the substrate was docked in orientations leading to hydroxylation at C_{19} or electron abstraction at C_{18} and C_{17}, and increased for other binding orientations to reach −250 kcal/mol in the case of oxidation at C_{14}. The results of 5 ps molecular dynamics simulations (Fig. 7) show that C_{18} remains fairly close to the ferryl oxygen, at a distance of about 4 Å, C_{17} is farther and methylene hydrogens at C_{16} move to a distance of more than 6 Å from the oxygen. Thus, electron abstraction at C_{18} should be easy, leading to 17(*R*),18(*S*) epoxidation. In contrast, oxidation at C_{16} would be difficult. In the case of C_{19}, methylene hydrogens remain within 3 Å from the heme oxygen thereby promoting EPA hydroxylation at this carbon, similar to the situation found for CYP1A1-bound AA. Higher yield of 17(*R*),18(*S*) epoxidation compared to 19-hydroxylation may be due to electronic factors. The results obtained for C_{20} were again very similar to those reported in the case of AA, and may be explained in the same way.

4. Discussion

In the current study we first time applied 'reconstituted CYP1A1 + reductase microsomes' to produce catalytically active CYP1A1 instead of the coexpression approach used in previous studies (e.g. [15,51]). While each approach for the reconstitution of enzymatic activity in CYP systems has unique advantages and disadvantages, the use of purified enzymes and natural control microsomes provides a broad range of flexibility. With respect to metabolic studies, this approach shares advantages of coexpression methods such as production of high levels of enzymatically active CYP enzymes in the natural microsomal membrane, the ability to control the CYP-to-P450 reductase ratio, and the ability to incorporate several CYP enzymes with P450 reductase (and/or cytochrome b_5) to study electron transfer and protein–protein interaction of the monooxygenase enzymes in their natural membrane environment. However, the availability of purified enzymes provides additionally the ability to perform structural and physicochemical experiments such as spectral binding studies to assess binding of substrates to CYP1A1 and to analyze effects of the membrane on enzymatic activity by incorporation of the purified enzymes into (artificial) lipid bilayers [52].

The present study shows for the first time that human CYP1A1 accepts both AA and EPA as substrates and efficiently converts these polyunsaturated fatty acids to specific sets of oxygenated metabolites. With AA, human CYP1A1 acts mainly as (ω − N) hydroxylase (N = 1–4) and produces a metabolite pattern distinct from that reported for purified rat CYP1A1 [32]. As shown in Fig. 2, both enzymes produce 19-OH-AA as the major metabolite and EET formation (mainly 14,15-EET) accounts only for approximately 7% of total products. The most striking difference in the regioselectivity of AA hydroxylation was the absence of any ω-hydroxylation by the human enzyme. A further species difference was noted comparing the relative amounts of 16-, 17-, and 18-OH metabolites which were produced in a molar ratio of about 1:0.6:2 by human CYP1A1, whereas a 1:2:2 ratio was reported for rat CYP1A1 [32]. Moreover, it is interesting to note that the AA metabolite profile produced by human CYP1A1 is clearly different from that reported for human CYP1A2 which acts primarily as an AA epoxygenase and forms 11,12-EET as major product [7].

The total activity of EPA oxidation by human CYP1A1 was comparable with that of AA metabolism. However, with EPA an epoxygenation reaction dominated which was almost completely directed towards the 17,18-double bond which distinguishes EPA from AA. Hydroxylation yielded preferentially 19-OH-EPA and as with AA, human CYP1A1 did not attack the terminal methyl group. Surprisingly, epoxygenation of the 17,18-double bond occurred not only with high regioselectivity but also with an almost absolute stereoselectivity in favor of producing the *R*,*S*-enantiomer. For comparison, a typical fatty acid ω-hydroxylase (rat CYP4A1), produced 17(*R*),18(*S*)-EETeTr as a minor product in addition to 20- and 19-OH-EPA and we found that the 17(*R*),18(*S*)- and 17(*S*),18(*R*)-enantiomers represented 64 and 36% of the total epoxygenation product [15]. Moreover, according to preliminary results, also well-known AA epoxygenases such as CYP2C8 and CYP2J2 do not display the high enantioselectivity of human CYP1A1 when epoxygenating EPA.[2] Modeling simulations with the human CYP1A1 homology model indicated that this might be due to unfavorable enzyme–substrate interactions when EPA is bound in a productive binding orientation leading to the *S*,*R*-enantiomeric product. Likewise, steric effects were apparently responsible for preferred oxidation of secobarbital at its si face by CYP2B1 [45].

As AA and EPA belong to different classes of fatty acids (AA is a (ω − 6) type fatty acid, whereas EPA is of (ω − 3) type), they behave differently in their metabolism by CYP1A1. Whereas CYP1A1 towards AA is mainly a hydroxylase, it acts primarily as epoxygenase towards EPA as substrate. This property is not limited to CYP1A1, but it is shared by other CYP isoforms, too, e.g. this was also found true for CYP2E1 which hydroxylates AA but epoxygenates linoleic acid, another (ω − 3) type fatty acid [53,54]. Additionally, CYP102 also exhibited this property as it is mainly an ω-hydroxylase for AA and a highly specific epoxygenase for EPA. Moreover, with eicosatrienoic acid as substrate, another (ω − 6) type fatty acid, CYP102 is again a pure hydroxylase [40]. One may speculate that possibly more such examples will be found in future studies. In structural terms, for both fatty acids tested here with CYP1A1, AA and EPA, the preferred sites for catalyzed oxygen insertion were the (ω − 1) and (ω − 2)

[2] W.-H. Schunck, unpublished work.

carbon atoms. It is therefore likely that both fatty acids occupy more or less similar spatial coordinates in the enzyme active site. Indeed our modeling provides evidence for lowest interaction energies of the fatty acid–CYP1A1 complexes when the substrates were docked in orientations leading to hydroxylation at C_{19} or electron abstraction at C_{18} and C_{17}. As discussed above, the reason is probably a hydrogen-bond network at the carboxy terminus bringing fatty acids of C_{20}-type in a position where the preferred sites for reactivity were the $(\omega - 1)$ and $(\omega - 2)$ carbon atoms.

There are some interesting parallels comparing the catalytic specificities of human CYP1A1 and bacterial CYP102. CYP102 shares with human CYP1A1 the exclusion of fatty acid ω-hydroxylation and the regioselectivity in EPA epoxygenation. Moreover, CYP102 also displays an almost absolute stereoselectivity in the epoxygenation of EPA to 17,18-EETeTr. However, in contrast to human CYP1A1 which produces the 17(*R*),18(*S*)-enantiomer, CYP102 produces exclusively the 17(*S*),18(*R*)-enantiomer. Both, the 17(*R*),18(*S*) and the 17(*S*),18(*R*) enantiomer, were generated by CYP1A1 and CYP102, respectively, with more than 99% optical purity.

As discussed above, neither human CYP1A1 nor CYP102 hydroxylate fatty acids at the ω-position, in contrast to the rat CYP1A1. In the case of CYP102, this may be due to the presence of Phe at position 87 in the active site, which blocks the ω-terminus of fatty acid substrates from approaching the heme thereby preventing ω-hydroxylation [40,44]. Thus, steric effects would govern the regiospecificity of fatty acid oxidation by this enzyme. In the case of human CYP1A1, which contains Ser-122 at the equivalent position, modeling studies indicated that, based on sterics, ω-hydroxylation of AA and EPA at C_{20} is as likely as highly efficient 19-hydroxylation, contrary to experimental results. This discrepancy may be explained by the demands of reaction energetics, since the energy barrier for the hydrogen abstraction at 1° carbon is higher than that at the 2° carbon. Recent studies [55] indicate that such energetic differences may be used to explain the regiospecificity of CYP-mediated reactions. In the case of the rat CYP1A1, which is able to hydroxylate AA at the ω-terminus, Ser-122 of the human enzyme is replaced with the Thr in the active site. Based on the sequence alignment, there are also other amino acid differences in the active site, which may alter its architecture and, consequently, enzyme–substrate interactions. Overall, both reactivity and steric effects would play a role in governing the regiospecificity of substrate oxidation.

It is interesting to compare binding of fatty acids in the active site of CYP1A1 to that of resorufin and benzo[*a*]-pyrene reported previously [43,48]. All substrates interact with the set of the same residues, although additional amino acids may interact with AA and EPA due to their larger size. These additional residues are mainly located in the substrate access channel, in the region of sheets 1–1 and 1–2, B–B′ loop and F–G loop. Moreover, while resorufin and benzo[*a*]pyrene are stabilized in the active site of CYP1A1 primarily by hydrophobic interactions [43], fatty acids are additionally stabilized at their carboxy termini by a fairly stable hydrogen bond network at the mouth of the substrate access channel. Such hydrogen bonds/ion pairs with the substrate carboxylate were reported for palmitoleic acid bound in the active site of CYP102 [44]. The substrate access channel residues that contributed to that hydrogen bond were Arg-47 and Tyr-51, which are equivalent to Thr-81 and Val-85 of CYP1A1, respectively, with Thr-81 involved in the formation of an analogous hydrogen bond network in CYP1A1. Thus, there seems to be a striking similarity between CYP1A1 and CYP102 in the mechanism of fatty acid binding and metabolism.

The capacity of aryl hydrocarbon-inducible CYP1A enzymes to metabolize AA and EPA may have physiological and toxicological consequences as first proposed by Rifkind *et al*. [34]. The main products of human CYP1A1 catalyzed AA hydroxylation (19-OH-AA) and EPA epoxygenation (17(*R*),18(*S*)-EETeTr) may influence the regulation of vascular tone as shown in animal models. 19-OH-AA was found to induce vasodilation in rabbit isolated perfused kidneys [56]. EPA epoxides, including 17,18-EETeTr, were reported to induce vasodilation in canine and porcine coronary microvessels [17]. In rat cerebral artery vascular smooth muscle cells, we observed a high degree of regio- and stereoselectivity comparing the effect of different EPA epoxides on BK channel activity and identified the 17(*R*),18(*S*)-EETeTr as the most effective compound [15]. Recently, also epoxides of docosahexaenoic acid (DHA; 22:6, $N - 3$) were shown to dilate porcine coronary arterioles and to activate BK channels over 1000 times more potent than observed for epoxide metabolites derived from AA [18]. Thus, it would be interesting to test whether CYP1A1 accepts docosahexaenoic acid as substrate, too. Taken together, these results indicate that the CYP-dependent metabolism of EPA and DHA is a source of physiologically active compounds which may contribute to the beneficial cardiovascular effects attributed to diets rich in these $(\omega - 3)$ polyunsaturated fatty acids such as fish oil. Interestingly, β-naphthoflavone treatment enhanced AA-induced vasorelaxation and bradykinin-induced formation of the endothelium-derived hyperpolarizing factor (EDHF) in several vascular beds [57–59]. However, recent studies clearly identified a β-naphthoflavone-inducible CYP2C as EDHF synthase in coronary arteries [60,61]. Thus, other CYP isoforms may dominate AA and EPA metabolism and the relative importance of CYP1A1 for the conversion of these polyunsaturated fatty acids to biologically active metabolites in the vasculature and other tissues remains to be established.

One further aspect is associated with the finding that 17(*R*),18(*S*)-EETeTr was reported to be metabolized to novel prostaglandins [62,63]. Therefore, biosynthesis of 17,18-epoxyprostaglandins in cells in which CYP1A1 is constitutively expressed and/or inducible should be con-

sidered to be affected by the CYP1A1-derived 17(*R*),18(*S*)-EETeTr when its biological effects are investigated.

Taken together, the present study demonstrates that AA and EPA can be efficiently metabolized by human CYP1A1. Remarkable features of these enzymatic activities of human CYP1A1 are (i) a clear preference for the hydroxylation of AA and EPA in (ω − 1) position, (ii) the absence of any hydroxylation of the terminal methyl groups of both substrates, and (iii) a nearly absolute regio- and stereoselectivity of EPA epoxygenation to 17(*R*),18(*S*)-EETeTr. Moreover, the capacity of human CYP1A1 to metabolize AA and EPA raises the possibility that its induction by polycyclic aromatic hydrocarbons may modulate or interfere with the production of physiologically active metabolites, in particular, in the cardiovascular system and the lung.

Acknowledgments

We are grateful to Dr. F.J. Gonzalez for providing CYP1A1 cDNA and virus for P450 reductase expression (National Cancer Institute, NIH, Bethesda, MD, USA) and to R. Zummach, C. Andreé and A. Sternke (all from Max Delbrueck Center for Molecular Medicine, Berlin-Buch) for assistance in HPLC and cell culturing. We thank Dr. R. Schmid (University Stuttgart, Germany) for a sample of bacterial CYP102 and Dr. M.L. Schwartzman (New York Medical College, Valhalla, NY, USA) for the CYP4A1 baculovirus. This work was supported by the German Research Foundation (DFG) grants RO 1287/2-3 (to I.R. and D.S.) and SCHU 822/3-1 (to W.-H.S.), the Volkswagen-Stiftung grant I/75 468 (to D.S.), and by the National Institutes of Health grants CA85542 and RR16440 (to G.D.S). Molecular modeling studies were performed at the Computational Chemistry and Molecular Modeling Laboratory, Department of Basic Pharmaceutical Sciences, School of Pharmacy, West Virginia University, Morgantown, WV.

References

[1] Capdevila JH, Falck JR, Harris RC. Cytochrome P450 and arachidonic acid bioactivation: molecular and functional properties of the arachidonate monooxygenase. J Lipid Res 2000;41:163–81.

[2] McGiff JC, Quilley J. 20-Hydroxyeicosatetraenoic acid and epoxyeicosatrienoic acids and blood pressure. Curr Opin Nephrol Hypertens 2001;10:231–7.

[3] Jacobs ER, Zeldin DC. The lung HETEs (and EETs) up. Am J Physiol Heart Circ Physiol 2001;280:H1–10.

[4] Zeldin DC. Epoxygenase pathways of arachidonic acid metabolism. J Biol Chem 2001;276:36059–62.

[5] Fleming I. Cytochrome P450 enzymes in vascular homeostasis. Circ Res 2001;89:753–62.

[6] Roman RJ. P-450 metabolites of arachidonic acid in the control of cardiovascular function. Physiol Rev 2001;82:131–85.

[7] Rifkind AB, Lee C, Chang TKH, Waxman DJ. Arachidonic acid metabolism by human cytochrome P450s 2C8, 2C9, 2E1, and 1A2: regioselective oxygenation and evidence for a role for CYP2C enzymes in arachidonic acid epoxygenation in human liver microsomes. Arch Biochem Biophys 1995;320:380–9.

[8] Zeldin DC, DuBois RN, Falck JR, Capdevila JH. Molecular cloning, expression and characterization of an endogenous cytochrome P450 arachidonic acid epoxygenase isoform. Arch Biochem Biophys 1995; 322:76–86.

[9] Wu S, Moomaw CR, Tomer KB, Falck JR, Zeldin DC. Molecular cloning and expression of CYP2J2, a human cytochrome P450 arachidonic acid epoxygenase highly expressed in heart. J Biol Chem 1996;271:3460–8.

[10] Bylund J, Kunz T, Valmsen K, Oliw EH. Cytochromes P450 with bisallylic hydroxylation activity of arachidonic and linoleic acids studied with human recombinant enzymes and with human and rat liver microsomes. J Pharmacol Exp Ther 1998;284:51–60.

[11] Powell PK, Wolf I, Jin R, Lasker JM. Metabolism of arachidonic acid to 20-hydroxy-5,8,11,14-eicosatetraenoic acid by P450 enzymes in human liver: involvement of CYP4F2 and CYP4A11. J Pharmacol Exp Ther 1998;285:1327–36.

[12] Lasker JM, Chen WB, Wolf I, Bloswick BP, Wilson PD, Powell PK. Formation of 20-hydroxyeicosatetraenoic acid, a vasoactive and natriuretic eicosanoid, in human kidney. J Biol Chem 2000;275:4118–26.

[13] Christmas P, Jones JP, Patten CJ, Rock DA, Zhen Y, Cheng S-M, Weber BM, Carlesso N, Scadden DT, Rettie AE, Soberman RJ. Alternative splicing determines the function of CYP4F3 by switching substrate specificity. J Biol Chem 2001;276:38166–72.

[14] Van Rollins M, Frade PD, Carretero OA. Oxidation of 5,8,11,14,17-eicosapantaenoic acid by hepatic and renal microsomes. Biochim Biophys Acta 1988;966:133–49.

[15] Lauterbach L, Barbosa-Sicard E, Wang M-H, Honeck H, Kärgel E, Theuer J, Schwartzman ML, Haller H, Luft FC, Gollasch M, Schunck W-H. Cytochrome P450-dependent eicosapentaenoic acid metabolites are novel BK channel activators. Hypertension 2002;39(Part II):609–13.

[16] Lu T, Van Rollins M, Lee H-C. Stereospecific activation of cardiac ATP-sensitive K^+ channels by epoxyeicosatrienoic acids: a structural determinant study. Mol Pharmacol 2002;62:1076–83.

[17] Zhang Y, Oltman CM, Lu T, Lee H-C, Dellsperger KC, Van Rollins M. EET homologs potently dilate coronary microvessel and activate BK(Ca) channels. Am J Physiol Heart Circ Physiol 2001;280:H2430–40.

[18] Ye D, Zhang D, Oltman C, Dellsperger K, Lee HC, VanRollins M. Cytochrome P450 epoxygenase metabolites of docosahexaenoate potently dilate coronary arterioles by activating large-conductance calcium-activated potassium channels. J Pharmacol Exp Therap 2002; 303:768–76.

[19] Pelkonen O, Nebert DW. Metabolism of polycyclic aromatic hydrocarbons: etiologic role in carcinogenesis. Pharmacol Rev 1982;34: 189–222.

[20] Guengerich FP. Metabolic activation of carcinogens. Pharmacol Ther 1992;54:17–61.

[21] Shimada T, Yun CH, Yamazaki H, Gautier JC, Beaune PH, Guengerich FP. Characterization of human lung microsomal cytochrome P450 1A1 and its role in the oxidation of chemical carcinogens. Mol Pharmacol 1992;41:856–64.

[22] Shimada T, Oda Y, Gillam EMJ, Guengerich FP, Inoue K. Metabolic activation of polycyclic aromatic hydrocarbons and other procarcinogens by cytochrome P450 1A1 and P450 1B1 allelic variant and other human cytochromes P450 in *Salmonella typhimurium* NM2009. Drug Metab Dispos 2001;29:1176–82.

[23] Ding XD, Kaminsky LS. Human extrahepatic cytochromes P450: function in xenobiotic metabolism and tissue-selective chemical toxicity in the respiratory and gastro-intestinal tracts. Annu Rev Pharmacol Toxicol 2003;43:149–73.

[24] Celander M, Weisbrod R, Stegemann JJ. Glucocorticoid potentiation of cytochrome P4501A1 induction by 2,3,7,8-tetrachlorodibenzo-*p*-dioxin in porcine and human endothelial cells in culture. Biochem Biophys Res Commun 1997;232:749–53.

[25] Dey A, Jones JE, Nebert DW. Tissue- and cell type-specific expression of cytochrome P450 1A1 and cytochrome P 450 1A2 mRNA in the mouse localized in situ hybridization. Biochem Pharmacol 1999;58: 525–37.
[26] Kerzee JK, Ramos KS. Constitutive and inducible expression of *Cyp1a1* and *Cyp1b1* in vascular smooth muscle cells: role of the Ahr bHLH/PAS transcription factor. Circ Res 2001;89:573–82.
[27] Zhao W, Ramos KS, Parrish AR. Constitutive and inducible expression of cytochrome P450IA1 and IB1 in human vascular endothelial and smooth muscle cells. In Vitro Cell Dev Biol Anim 1998;34:671–3.
[28] Schwarz D, Kisselev P, Schunck W-H, Chernogolov A, Boidol W, Cascorbi I, Roots I. Allelic variants of human cytochrome P450 1A1 (CYP1A1): effect of T461N and I462V substitutions on steroid hydroxylase specificity. Pharmacogenetics 2000;10:519–30.
[29] Zhang Q-Y, Dunbar D, Kaminsky L. Human cytochrome P-450 metabolism of retinals to retinoic acids. Drug Metab Dispos 2000; 28:292–7.
[30] Chernogolov A, Behlke J, Schunck W-H, Roots I, Schwarz D. Human CYP1A1 allelic variants: baculovirus expression and purification, hydrodynamic, spectral, and catalytical properties and their potency in the formation of all-*trans*-retinoic acid. Prot Expr Purif 2003;28:259–69.
[31] Oliw EH, Guengerich FP, Oates JA. Oxygenation of arachidonic acid by hepatic monooxygenases. Isolation and metabolism of four epoxide intermediates. J Biol Chem 1982;257:3771–81.
[32] Falck JR, Lumin S, Blair I, Dishman E, Martin MV, Waxman DJ, Guengerich FP, Capdevila JH. Cytochrome P-450-dependent oxidation of arachidonic acid to 16-, 17-, and 18-hydroxyeicosa-tetraenoic acids. J Biol Chem 1990;265:10244–9.
[33] Rifkind AB, Kanetoshi A, Orlinick J, Capdevila JH, Lee C. Purification and biochemical characterization of two major cytochrome P-450 isoforms induced by 2,3,7,8-tetrachlorodibenzo-*p*-dioxin in chick embryo liver. J Biol Chem 1994;269:3387–96.
[34] Rifkind AB, Gannon M, Gross SS. Arachidonic acid metabolism by dioxin-induced cytochrome P-450: a new hypothesis on the role of P-450 in dioxin toxicity. Biochem Biophys Res Commun 1990;172: 1180–8.
[35] Schlezinger JJ, Parker C, Zeldin DC, Stegemann JJ. Arachidonic acid metabolism in the marine fish *Stenotomus chrysobs* (Scup) and the effects of cytochrome P450 1A inducers. Arch Biochem Biophys 1998;353:265–75.
[36] Tamura S, Korzekwa KR, Kimura S, Gelboin HV, Gonzalez FJ. Baculovirus-mediated expression and functional characterization of human NADPH-P450 oxidoreductase. Arch Biochem Biophys 1992; 293:219–23.
[37] Buters JTM, Shou M, Hardwick JP, Korzekwa KR, Gonzalez FJ. cDNA-directed expression of human cytochrome P450 CYP1A1 using baculovirus. Drug Metab Dispos 1995;23:696–701.
[38] Omura T, Sato R. The carbon monoxide-binding pigment of liver microsomes. J Biol Chem 1964;239:2370–8.
[39] Yasukochi Y, Masters BS. Some properties of detergent-solubilized NADPH-cytochrome *c* (cytochrome P450) reductase purified by biospecific affinity chromatography. J Biol Chem 1976;251:5337–44.
[40] Capdevila JH, Wei S, Helvig C, Falck JR, Belosludtsev Y, Truan G, Graham-Lorence SE, Peterson JA. The highly stereoselective oxidation of polyunsaturated fatty acids by cytochrome P450BM-3. J Biol Chem 1996;271:22663–71.
[41] Paulsen MD, Ornstein RL. A 175 psec molecular dynamics simulation of camphor-bound cytochrome P-450cam. Proteins 1991;11:184–204.
[42] Paulsen MD, Ornstein RL. Predicting the product specificity and coupling of cytochrome P450cam. J Comput Aided Mol Des 1992;6:449–60.
[43] Szklarz GD, Paulsen MD. Molecular modeling of cytochrome P450 1A1: enzyme–substrate interactions and substrate binding affinities. J Biomol Struct Dyn 2002;20:155–62.
[44] Li H, Poulos TL. The structure of the cytochrome p450BM-3 haem domain complexed with the fatty acid substrate, palmitoleic acid. Nat Struct Biol 1997;4:140–6.
[45] He K, He YA, Szklarz GD, Halpert JR, Correia MA. Secobarbital-mediated inactivation of cytochrome P450 2B1 and its active site mutants. J Biol Chem 1996;271:25864–72.
[46] Kent UM, Hanna IH, Szklarz GD, Vaz NAD, Halpert JR, Bend JR, Hollenberg PF. Significance of glycine 478 in the metabolism of *N*-benzyl-1-aminobenzotriazole to reactive intermediates by cytochrome P450 2B1. Biochemistry 1997;36:11707–16.
[47] Szklarz GD, Halpert JR. Molecular modeling of cytochrome P450 3A4. J Comput Aided Mol Des 1997;11:265–72.
[48] Liu J, Ericksen SS, Besspiata D, Fisher CW, Szklarz GD. Characterization of substrate binding to cytochrome P450 1A1 using molecular modeling and kinetic analyses: case of residue 382. Drug Metab Dispos 2003;31:412–20.
[49] Strobel SM, Szklarz GD, He YQ, Foroozesh M, Alworth WL, Roberts ES, Hollenberg PF, Halpert JR. Identification of selective mechanism-based inactivators of cytochromes P-450 2B4 and 2B5, and determination of the molecular basis for differential susceptibility. J Pharmacol Exp Ther 1999;290:445–51.
[50] Guo Z, Gillam EM, Ohmori S, Tukey RH, Guengerich FP. Expression of modified human cytochrome P450 1A1 in *Escherichia coli*: effects of 5′ substitution, stabilization, purification, spectral characterization and catalytic properties. Arch Biochem Biophys 1994;312:436–46.
[51] Schwarz D, Kisselev P, Cascorbi I, Schunck WH, Roots I. Differential metabolism of benzo[*a*]pyrene and benzo[*a*]pyrene-7,8-dihydrodiol by human CYP1A1 variants. Carcinogenesis 2001;22:453–9.
[52] Kisselev P, Schwarz D, Platt KL, Schunck WH, Roots I. Epoxidation of benzo[*a*]pyrene-7,8-dihydrodiol by human CYP1A1 in reconstituted membranes: effects of charge and nonbilayer propensity of the membrane. Eur J Biochem 2002;269:1799–805.
[53] Laethem RM, Balazy M, Falck JR, Laethem CL, Koop DR. Formation of 19(*S*)-, 19(*R*)-, and 18(*R*)-hydroxyeicosatetraenoic acids by alcohol-inducible cytochrome P450 2E1. J Biol Chem 1993;268:12912–8.
[54] Moran JH, Mitchell LA, Bradbury JA, Qu W, Zeldin DC, Schnellmann RG, Grant DF. Analysis of the cytotoxic properties of linoleic acid metabolites produced by renal and hepatic P450s. Toxicol Appl Pharmacol 2000;168:268–79.
[55] Higgins L, Korzekwa KR, Rao S, Shou M, Jones JP. An assessment of the reaction energetics for cytochrome P450-mediated reactions. Arch Biochem Biophys 2001;385:220–30.
[56] Carrol MA, Balazy Y, Margiotta P, Huang DD, Falck JR, McGiff JC. Cytochrome P-450-dependent HETEs: profile of biological activity and stimulation by vasoactive peptides. Am J Physiol 1996;271(4Pt2): R863–9.
[57] Pinto A, Abraham NG, Mullane KM. Arachidonic acid-induced endothelial-dependent relaxations of canine coronary arteries: contribution of a cytochrome P-450-dependent pathway. J Pharmacol Exp Ther 1987;240:856–63.
[58] Oyekan AO, McGiff JC, Quilley J. Cytochrome P-450-dependent vasodilation of rat kidney by arachidonic acid. Am J Physiol 1991; 261(3Pt2):H714–9.
[59] Popp R, Bauersachs J, Hecker M, Fleming I, Busse R. A transferable beta-naphthoflavone-inducible, hyperpolarizing factor is synthesized by native and cultured porcine coronary endothelial cells. J Physiol 1996;497.3:699–709.
[60] Fisslthaler B, Popp R, Kiss L, Potente M, Harder DR, Fleming I, Busse R. Cytochrome P450 2C is an EDHF synthase in coronary arteries. Nature 1999;401:493–7.
[61] Fisslthaler B, Fleming I, Busse R. EDHF: a cytochrome P450 metabolite in coronary arteries. Semin Perinatol 2000;24:15–9.
[62] Oliw EH. 17*R*(18*S*)epoxyeicosatetraenoic acid, a cytochrome P450 metabolite of 20:5N − 3 in monkey seminal vesicles, is metabolized to novel prostaglandins. Biochem Biophys Res Commun 1991;178: 1444–50.
[63] Oliw EH. Oxygenation of polyunsaturated fatty acids by cytochrome P450 monooxygenases. Prog Lipid Res 1994;33:329–54.